S. Mohammad Ali Banijamali
Department of Mechanical
and Industrial Engineering,
Northeastern University,
Boston, MA 02115

Ramin Oftadeh
Department of Mechanical
and Industrial Engineering,
Northeastern University,
Boston, MA 02115;
Center for Advanced Orthopaedic Studies,
Department of Orthopaedic Surgery,
Beth Israel Deaconess Medical Center,
Harvard Medical School,
Boston, MA 02215

Ara Nazarian
Center for Advanced Orthopaedic Studies,
Department of Orthopaedic Surgery,
Beth Israel Deaconess Medical Center,
Harvard Medical School,
Boston, MA 02215

Ruben Goebel
Sport Science Program,
Qatar University,
Doha 2713, Qatar

Ashkan Vaziri
Department of Mechanical
and Industrial Engineering,
Northeastern University,
Boston, MA 02115

Hamid Nayeb-Hashemi[1]
Professor of Mechanical Engineering
Department of Mechanical
and Industrial Engineering,
Northeastern University,
334 Snell Engineering Center,
360 Huntington Avenue,
Boston, MA 02115
e-mail: hamid@coe.neu.edu

Effects of Different Loading Patterns on the Trabecular Bone Morphology of the Proximal Femur Using Adaptive Bone Remodeling

In this study, the changes in the bone density of human femur model as a result of different loadings were investigated. The model initially consisted of a solid shell representing cortical bone encompassing a cubical network of interconnected rods representing trabecular bone. A computationally efficient program was developed that iteratively changed the structure of trabecular bone by keeping the local stress in the structure within a defined stress range. The stress was controlled by either enhancing existing beam elements or removing beams from the initial trabecular frame structure. Analyses were performed for two cases of homogenous isotropic and transversely isotropic beams. Trabecular bone structure was obtained for three load cases: walking, stair climbing and stumbling without falling. The results indicate that trabecular bone tissue material properties do not have a significant effect on the converged structure of trabecular bone. In addition, as the magnitude of the loads increase, the internal structure becomes denser in critical zones. Loading associated with the stumbling results in the highest density; whereas walking, considered as a routine daily activity, results in the least internal density in different regions. Furthermore, bone volume fraction at the critical regions of the converged structure is in good agreement with previously measured data obtained from combinations of dual X-ray absorptiometry (DXA) and computed tomography (CT). The results indicate that the converged bone architecture consisting of rods and plates are consistent with the natural bone morphology of the femur. The proposed model shows a promising means to understand the effects of different individual loading patterns on the bone density. [DOI: 10.1115/1.4029059]

Keywords: human femur, finite element analysis, trabecular bone, rod, plate, walking, stair climbing, stumbling without falling

Introduction

Bone is a living tissue which undergoes continuous change. There are three types of cells in the bone which are responsible for the changes in bone structure: osteocytes, osteoclasts and osteoblasts. Osteoclasts are a group of cells which resorb the bone. Osteoblasts are cells that form the bone, and osteocytes, also called resting osteoblasts, reside in bone permanently. It is reported that 10–15% of the bone in the body is replaced with the new bone every year [1].

Wolff et al. proposed that every change in the internal structure of bone is in response to external loads, and that healthy bone adapts to the loads it bears [2]. This statement is known as Wolff's law or the law of bone remodeling. Many researchers have investigated and tried to refine this law using computational and finite element methods (FEM). In one of the early FEM studies, Brekelmans et al. obtained stress and deformation in a 2D model of proximal femur by applying forces at the femoral head and greater trochanter [3]. However, there was no attempt to relate this information to bone density or to develop an adaptive bone remodeling model. Several investigators have used 2D FEM results to develop a mathematical model to predict bone architecture (adaptive bone remodeling) using various stimuli including strain and stress history [4]. Carter et al. related local bone apparent density to loading history and concluded that bone density is adjusted in response to local strain energy density or strength [5]. In another study, they used a stress based remodeling theory to predict the distribution of bone density and trabecular structure morphology in a 2D model of proximal femur [5]. The apparent density and material properties of each element was changed based on stress stimulus for each element. Strain energy density has also been used as a feedback control to predict bone structure and its density in a 2D model of proximal femur with an intramedullary prosthesis; it is shown that the amount of bone resorption depends mainly on the rigidity and the bonding characteristics of the implant [6]. Marzban et al. developed an efficient strain

[1]Corresponding author.

Manuscript received August 8, 2014; final manuscript received November 7, 2014; accepted manuscript posted November 13, 2014; published online December 10, 2014. Assoc. Editor: Blaine Christiansen.

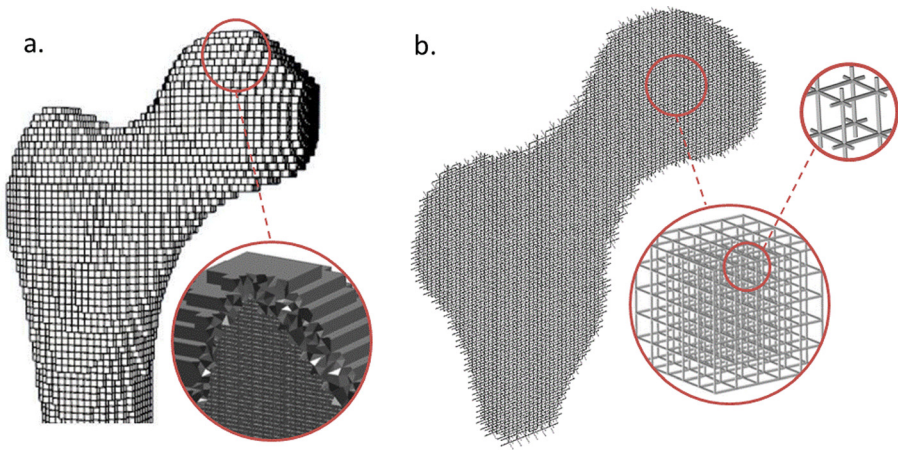

Fig. 1 Initial model of proximal femoral head before the start of the remodeling process: (*a*) Cortical bone and (*b*) trabecular bone structure

energy based remodeling method which converges in fewer number of iterations and therefore requires less computational time [7]. In their model, strain energy density was obtained using loading data in a gait cycle. Three-dimensional (3D) models of bone have also been developed, and bone adaptation has been investigated. Bitsakos et al. have investigated the effect of muscle loading on bone remodeling simulations around hip implants. In their remodeling algorithm, changes in total strain energy density were used as the stimulus. They concluded that it is advantageous to include muscle loading in models when assessing bone density changes around implants [8]. Turner et al. developed a 3D FEM model of proximal femur to predict the alterations in periprosthetic apparent density [9]. They used muscle and joint loads from 45% of the gait cycle and used strain as the stimulus in their adaptive remodeling investigation. Despite some differences at specific regions, the trends were consistent with the clinically found density distribution. Boyle and Kim [10] used design space optimization in their trabecular bone remodeling of the proximal femoral head. They used a microfinite element 3D model of the femur and two load cases of walking and stair climbing in their simulations. By minimizing the strain energy in the structure, their results for bone density distribution and trabecular trajectories showed a good agreement with that of natural bone. Hambli et al. investigated human proximal femur remodeling along with its fracture behavior and showed that bone remodeling data can potentially predict fracture risk [11]. Fyhrie and Carter proposed an optimization mathematical theory which relates local equivalent stress to bone apparent density and predicted bone density distribution in a 3D model of the femur [12,13]. Adachi et al. used stress as a stimulus in adaptive bone remodeling of a 2D model of the femur [14]. They considered nonuniformity of stress distribution on the cancellous bone surface as the stimulus in the remodeling process and showed that their proposed model can predict the optimal structure of bone. Adachi et al. used a similar theory for a 3D voxel based finite element model of cancellous bone [15]. The changes in the structure were made by addition and removal of voxel elements to/from the trabecular surface. A time-dependent theory for bone remodeling was proposed by Beaupré et al. [16]. The changes in local bone density were evaluated thorough consideration of bone surface areas available for osteoblastic and osteoclastic activities.

It has been shown that bone is an anisotropic material mainly due to the trabecular bone structure [17], and the anisotropy is mainly due to the trabecular bone structure [18]. Several studies have modeled the bone as an orthotropic material [17,19–21] and also transversely isotropic material [22].

The 3D remodeling rule developed in this study is an extension to our previous 2D model of the proximal femur [23]. The basis of the proposed remodeling technique is to keep the structure's local maximum principal stress in a defined stress range. This is achieved by adding bone (i.e., increasing diameter of the connecting rods) and removing structural elements in the locations where stress is higher and lower than the admissible stress range, respectively. Maximum principal stress was previously used to predict the ultimate fracture load of bone tissue by Keyak et al. with less than 30% error [24]. The cube-like uniform structure designed for trabecular bone in this study and the use of beam elements makes two of the principal stresses negligible in comparison with the other one. Therefore, the maximum principal stress criterion was used here for bone remodeling. The optimum stress range is obtained by comparing the density distribution with those obtained experimentally. Also, in our adaptive bone density remodeling, we have modeled bone tissue material as both isotropic and transversely isotropic materials and have compared the corresponding results. Therefore, the purpose of this study is to provide a reliable, fast and simple computational method to predict the internal architecture distribution of bone, as well as to understand the effects of different loading conditions on the bone density distribution in a proximal femur. *We hypothesize that the proposed model can capture the creation of trabecular plates which are important load-bearing elements and have been rarely addressed in previous studies*. Furthermore, a realistic representation of the trabecular bone can be developed based on this model consisting of a network of rods and plates.

Methods

Modeling of the Femur. A 3D FEM model of the femur was constructed from a subject specific CT image consisting of two separate regions: trabecular and cortical bones. CT images which are in Digital Imaging and Communications in Medicine (DICOM) formats were obtained from the VAKHUM project public database which can be found in this website.[2] The image slices have 1 mm thickness in the epiphysis and 3 mm thickness in the diaphysis. The cortical bone was considered as a solid material (Fig. 1(*a*)), and the trabecular part was made up of a network of interconnected rods (Fig. 1(*b*)). Since the majority of the loads exerted on the femur are in the anatomic direction (i.e., hip joint load), trabecular plates were mainly formed in that direction. For this reason, a cubical frame structure was used in our simulation to capture the natural structure of trabecular bone. In contrast, the use of a tetrahedron structure in our primary investigations resulted in the formation of angled plates which is not realistic.

[2]http://www.ulb.ac.be/project/vakhum/index.html

The solid cortical bone encompassing the trabecular bone had two important roles: (1) retain the natural structure of the femur and (2) allow for contact and muscle forces to be applied at specific locations and prevent discontinuities in the converged solution. The initial cubical frame structure to simulate trabecular bone structure consisted of cubes with dimensions of $2 \times 2 \times 2$ mm. The connecting beam elements in each cube had circular cross sections with an initial radius of 0.1 mm. The mean radius of the trabecular rods have been reported to be 0.2 mm [25]. However, here we select a lower value initially to let the adaptation algorithm optimize the trabecular bone architecture. Elements with the length of 2 mm were used to capture the porosity in the bone. The initial trabecular frame structure consisted of approximately 43,000 rods which was optimized subsequently during the adaptation process. Rods in trabecular structure were modeled as transversely isotropic. For transversely isotropic material properties we used $E_1 = 19.9$ GPa, $E_2 = 11.9$ GPa, $\nu_{12} = 0.385$, $\nu_{23} = 0.442$, and $G_{12} = 5.2$ GPa in our model while 1 indicates the axial direction for rods. These data are taken from the works of Couteau et al. and Taylor et al. [26,27]. Simulation was also carried out using homogeneous isotropic material properties for the purpose of comparison with elastic properties of $E = 19.9$ GPa and $\nu = 0.3$. Cortical bone was considered isotropic for both cases with $E = 19.9$ GPa, and $\nu = 0.3$.

Loading Profiles. Walking, stair climbing and stumbling without falling loading profiles were used to simulate adaptive bone remodeling. Walking and stair climbing loading data were obtained from the work of Heller et al. [28]. They used the lower extremity model and gait data to find hip contact and muscle forces. Muscle forces were obtained by grouping the muscles with similar functions. The values of the loads at the instant of peak hip contact force for both activities, which were around midstance, were used in the simulations.

For the case of "stumbling without falling" loading, the data obtained by El'Sheikh et al. was used in the simulations [29]. For joint loads, El'Sheikh et al. derived their data from a previous study [30] in which telemetering total hip prostheses was used to measure loading patterns of the hip joint. Hip joint loading was reported at 58% of the gait cycle, where it was at its peak. For muscle loads, El'Sheikh et al. used a simplified set of muscle loads at 85% of the gait cycle, which were derived from the work of Lennon et al. [31]. We normalized all forces by multiplying them to the ratio of the subject's weight in that study to the weight of the subject in the current study. Table 1 shows the hip contact and muscle forces in percentage of body weight. The 3D view of model with muscle attachment sites and the direction of coordinates is displayed in Fig. 2.

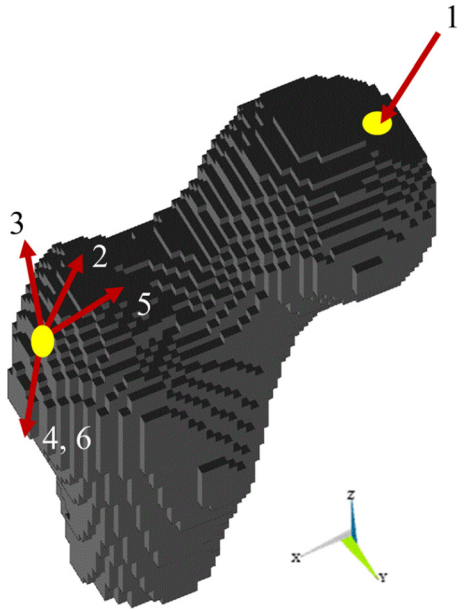

Fig. 2 3D model of femur with muscle attachment sites and the direction of forces and coordinate system. (1) Hip contact, (2) abductor, (3) tensor fascia latae, proximal part, (4) tensor fascia latae, distal part, (5) ilio-tibial tract, proximal part, and (6) ilio-tibial tract, distal part. The magnitudes of forces for the three cases of loadings are shown in Table 1.

Remodeling Method. It has been shown that both trabecular and cortical bone adapt to external stimuli; however, trabecular bone remodeling is more active than cortical bone (26% turnover rate in trabecular bone vs. 3% in cortical bone) [17]. In this study, only trabecular bone remodeling was investigated, and the cortical bone remained unchanged during the remodeling process.

ANSYS (v. 14.0, ANSYS Inc., Canonsburg, PA) commercial software package was used to simulate bone adaptation. The cortical part of the model was meshed with 3D solid 10 node tetrahedron elements (SOLID187) with a quadratic displacement behavior, well suited for modeling irregular geometries. Trabecular rods were meshed with BEAM188, which is a 2 node 3D element, suitable for analyzing slender to moderately stubby/thick beam structures. This element is based on the Timoshenko beam theory and shear deformation effects are included in the beam calculations. There is an independent coordinate system on each element which defines the direction of the elastic material properties for the case of a transversely isotropic material.

Table 1 Muscle and joint contact forces in percentage of body weight [28,29]

Activity	Force name (force number[a])	X[b]	Y[b]	Z[b]	Site
Walking	Hip contact (1)	54	−32.8	−229.2	Femoral head
	Abductor (2)	−58	4.3	86.5	Greater trochanter
	Tensor fascia latae, proximal part (3)	−7.2	11.6	13.2	Greater trochanter
	Tensor fascia latae, distal part (4)	0.5	−0.7	−19	Greater trochanter
Stair climbing	Hip contact (1)	59.3	−60.6	−236.3	Femoral head
	Abductor (2)	−70.1	28.8	84.9	Greater trochanter
	Tensor fascia latae, proximal part (3)	−3.1	4.9	2.9	Greater trochanter
	Tensor fascia latae, distal part (4)	0.2	−0.3	−6.5	Greater trochanter
	Ilio-tibial tract, proximal part (5)	−10.5	3	12.8	Greater trochanter
	Ilio-tibial tract, distal part (6)	0.5	−0.8	−16.8	Greater trochanter
Stumbling	Hip contact	319.1	−97.6	−797.7	Femoral head
	Abductor, Gluteus minimus (2)	−40.7	39.2	19.5	Greater trochanter
	Abductor, Gluteus medius (2)	−37.7	23.3	46.5	Greater trochanter
	Ilio-tibial band (5, 6)	−8.6	−10.8	−8.4	Greater trochanter

[a]Force numbers which are depicted in Fig. 2.
[b]Percentage of body weight.

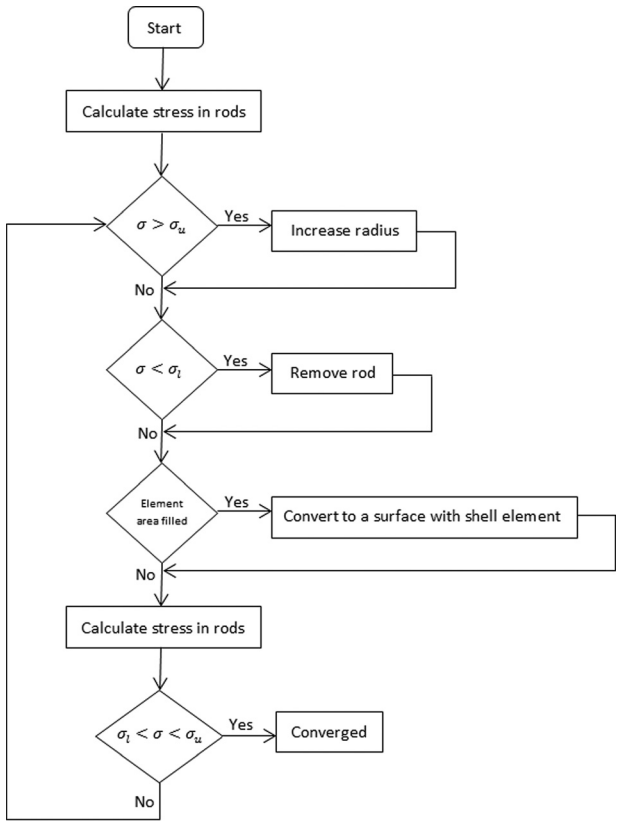

Fig. 3 Schematic flow chart of the remodeling process

For the remodeling process, an ANSYS Parametric Design Language (APDL) code was developed. Figure 3 shows an overview of the proposed remodeling process. The main goal of the program was to keep the stress (σ) in the trabecular bone rods in a predefined range. The program starts by determining the stresses in the all rods. Then, if the maximum principal stress is higher than an upper level ($\sigma > \sigma_u$), the radius of the rod is increased. If the maximum principal stress is less than a lower bound ($\sigma < \sigma_l$), the link is deleted. The program also keeps track of the spacing between rods and turns faces of the cubes into an area if the face is filled due to the increase in the radius of rods. The generated area is then meshed with a shell element and the developed square shell will have the thickness of the mean diameter of the edges of that square. The problem was solved iteratively until all conditions were satisfied, which was to maintain the maximum principal stress in all of the rods in the defined range.

In order to start the remodeling process, an upper (σ_u) and lower (σ_l) stress limit in rods had to be chosen. In this study, the upper boundary was set to the maximum reported yield stress values of 10 MPa [32]. Homminga et al. used a combination of compression testing and microfinite element analysis to calculate mechanical properties of the femur cancellous bone in the order of 1 mm and reported a yield stress of 6.7 ± 2.7 MPa [32]. Our choice was based on the fact that the yield stress of bone decreases with age; therefore, a higher value was selected to consider a normal age case. Lower bound was set to 1.5 MPa which is arbitrarily selected based on the comparison of the converged solution with one obtained from DXA. Also various lower and upper bounds were selected to understand their effects on the converged bone density which are discussed in detail in the Results section.

Results

The initial distribution of the maximum principal stress in the trabecular bone architecture before adaptation remodeling, which initially contains only rods under: (a) walking, (b) stair climbing, and (c) stumbling without falling load, is compared in Fig. 4. It can be seen that the regions with high stresses should get denser to withstand the changes in the loading in the structure. The initial radius of the rods is set to 0.1 mm, which was changed during the remodeling process. Four groups of loads in the internal structure of the femur, which are principal compressive, principal tensile, secondary compressive and secondary tensile, shaped the architecture of trabecular bone (here primary and secondary are defined as component of trabecular bone carrying the major load applied to the structure, and secondary is defined as components carrying load at least an order of magnitude less than primary components). Also, there was a triangular region known as Ward's triangle, which had the lowest density. These patterns are highlighted in Fig. 5 along with the location of Ward's triangle.

The results of three loading cases, based on the criterion of [1.5, 10] MPa stress, are shown in Fig. 5. It is noteworthy that in this figure, the cortical part of the bone is removed, and only trabecular bone structure, which was subjected to adaptation, is shown. Higher and lower values were also selected for the maximum and minimum stress level, in order to understand their effects on the converged solution. Also as the loads on femur increased, so did bone density. In the stumbling case, where the applied load to the femur was higher than the other loading cases, the density in the converged model was the highest compared with the two other cases, and it was the only case in which trabecular plates were formed in the femoral neck. 3D views of the created plates during the remodeling process are displayed in Fig. 6. The location of the trabecular plates can be observed in this figure.

Discussion and Conclusion

A novel adaptive bone remodeling rule was proposed to capture proximal bone architecture. In contrast to previous studies, where bone was considered as a continuous medium, this study

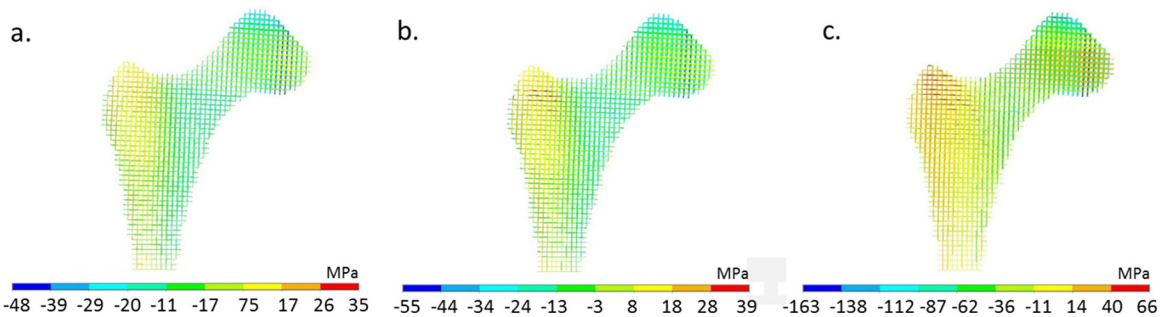

Fig. 4 Maximum principal stress contour in trabecular bone before adaptation process: (*a*) walking, (*b*) stair climbing, and (*c*) stumbling

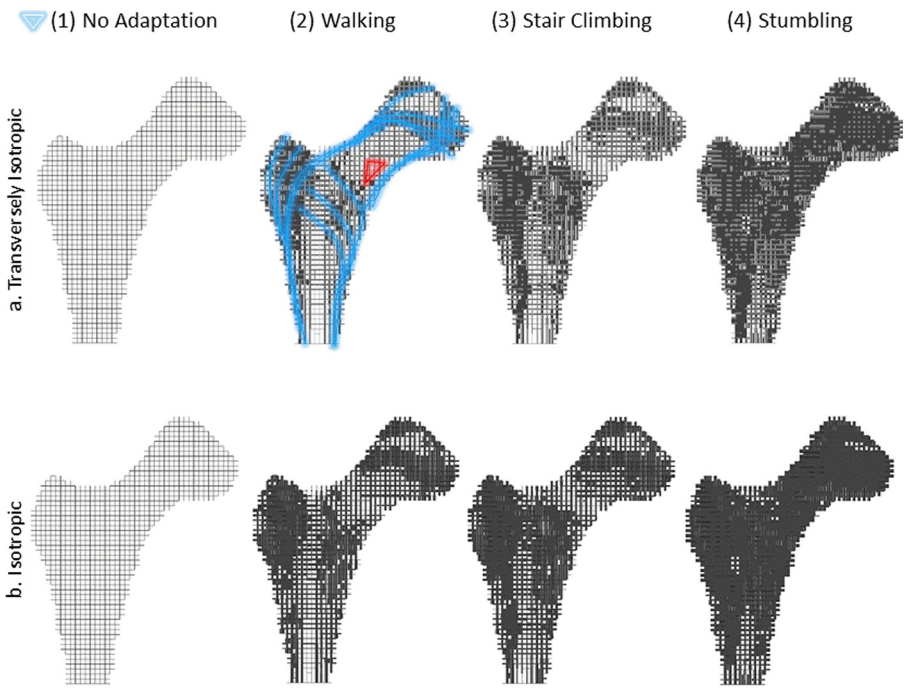

Fig. 5 Side views of converged trabecular structure for the stress range criteria of [1.5, 10] MPa (*a*) modeling material as transversely isotropic and (*b*) modeling material as isotropic. On the case of walking with transversely isotropic material, curved overlays indicate patterns of trabecular bone created in the direction of principal and secondary loading groups and the triangle at the femoral neck shows the Ward's triangle.

considered trabecular bone as a cubical frame structure with interconnected rods and plates. The scale of intratrabecular spacing in cancellous bone has been reported to be of the order of 1 mm^3 [18]. Our choice of 2 mm elements substantially reduced computation time in comparison with using 1 mm elements. The computational time is greatly decreased in the present approach for simulation of the trabecular remodeling. For example, Boyle and Kim [10] used a higher resolution voxel based model which required 342.9 h of computational time while our models needed between 5 and 9 h of computation time (depending on the loading case) for convergence on a regular computer with Intel Xeon W3550 @ 3.07 GHz processor. The cortical bone model also had a cubic look, which was designed in a way to require fewer elements for precise and less error-prone meshing (Fig. 1). Cubical computational models of the femur have been used previously for prediction of femoral fractures [24,33]. The model allows for the formation of plates in the loading direction upon completion of simulations as observed in trabecular bones.

Two material models were considered for the proposed model, transversely isotropic and isotropic. The simulations were performed for three loading cases: two regular daily activities and one with excessive pressure on the femur. The results showed negligible effect of the material properties in the converged density distribution for isotropic and transversely isotropic cases (Fig. 5). Furthermore, the bone density distribution pattern seemed to be similar. This confirms that the architecture of trabecular bone plays a significant role in determining anisotropic or orthotropic behavior of the bone at the macroscopic scale, which is also confirmed by other studies [34–38].

Our remodeling concept was based on allowable stress range in the proximal femur. Figure 7 shows the cross section of femur upon convergence for different stress ranges for walking and stair climbing. The material elastic properties are considered to be

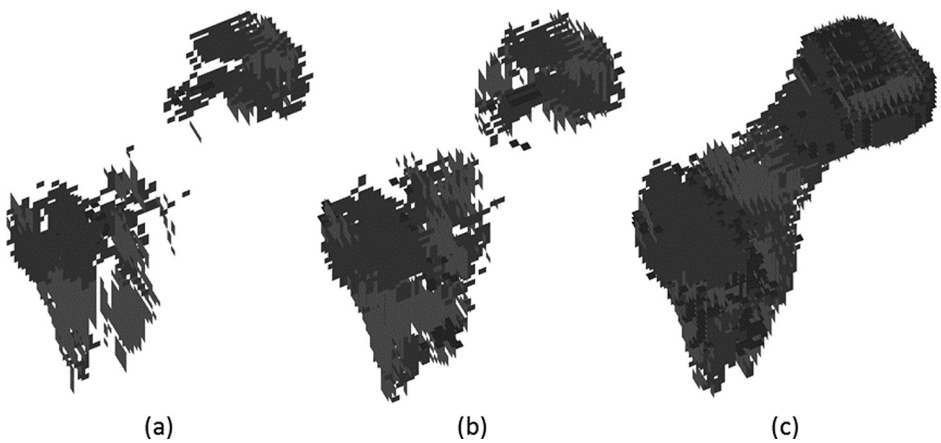

Fig. 6 3D view of trabecular plates—bone subjected to (*a*) walking, (*b*) stair climbing, and (*c*) stumbling. For all the cases the transversely isotropic material has been used.

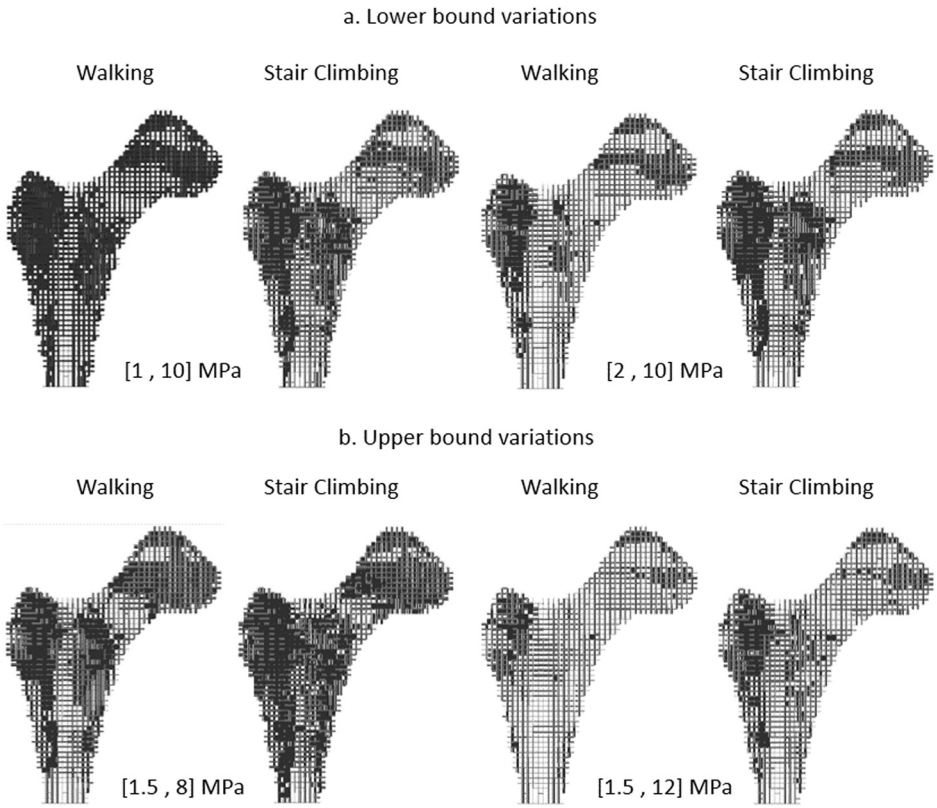

Fig. 7 Final architecture of trabecular bone showing the effect of various stress ranges on converged model for walking and stair climbing load cases. With (*a*) lower bound variations and (*b*) upper bound variations.

transversely isotropic. Figure 7 shows that decreasing the maximum stress limit leads to over densification. On the other hand, increasing the lower and upper bounds resulted in creation of excessive porosity, where no trabecular plates were made in the structure. This suggests that the allowable stress range can be optimized by comparing the converged results with actual bone density. The optimum stress range of [1.5, 10] MPa used in this investigations was based on the direct comparison of the converged density distribution and those obtained using DXA and our previous work [23].

Bone volume fraction was evaluated at the three regions of the proximal femur, namely, femoral head, femoral neck and trochanter for the walking case and using stress range of [1.5, 10] MPa. Bone volume fraction was defined as the ratio of the bone tissue volume to the total bone volume. Figure 8 shows the regions used to obtain bone volume fraction. Bone volume fraction was compared with those obtained by Baum [39] and Boyle and Kim [10] (Table 2). Additionally, bone density ratio in these regions was compared with data from Huber et al. [40] (Table 2). Our results indicated a high density region in the femoral head and a low density region in the femoral neck. Also, the low density medullary cavity was predicted in the converged models. According to Table 2, our model predicted slightly higher bone volume fraction than normal bone volume fraction for the trochanter region. Apart from that, other regions were in good agreement with natural volume fractions reported by other studies [39].

Trabecular plates are important structural elements since they bear higher amount of loads compared with rods. As the majority of the loads exerted on the femur are vertical loads, many vertical plates can be seen in the trabecular bone structure. The proposed model was designed to display load-bearing plates. Figure 6 shows the 3D plots of created plates in the femur for walking, stair climbing and stumbling loading cases with transversely isotropic material properties. As seen in this figure, for the cases of walking and stair climbing the creation of plates was mostly in the femoral head and trochanter region, and no trabecular plates were created in the neck. Only in the case of stumbling, trabecular plates were created in the femoral neck region, due to the extremely high magnitude of loads exerted on the femur during stumbling.

Comparing bone architecture for the three different loading scenarios indicated that the higher magnitude loads imposed by the abductors, attached to the greater trochanter, during stair climbing when compared to walking, resulted in higher densities in the center and even around the neck of femur. The excessive loads during

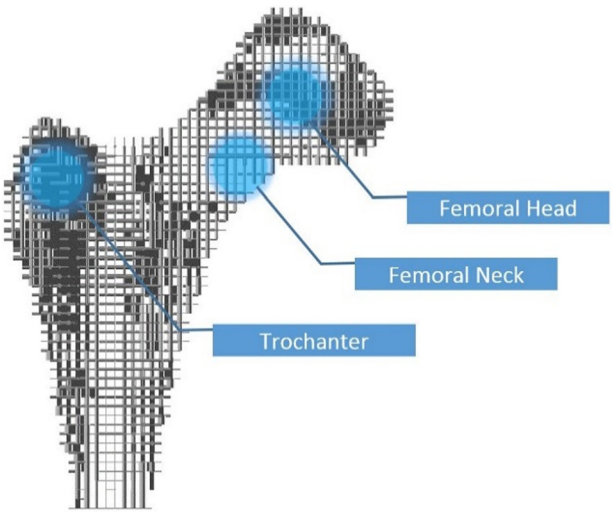

Fig. 8 Head, neck, and trochanter regions used to obtain bone volume fractions (BV/TV)

Table 2 Comparison of bone volume fraction of selected regions (Fig. 8) in this study with other studies

Region	This study (BV/TV)	(Baum et al. [39]) (BV/TV)	(Huber et al. [40]) BMD (mg/cm^3)	(Boyle and Kim [10]) (BV/TV)
Head	0.557	0.55 ± 0.14	224 ± 60.4	0.323
Trochanter	0.230	0.15 ± 0.10	74.6 ± 45.3	0.217
Neck	0.124	0.10 ± 0.09	43.5 ± 52.4	0.061
Head/trochanter ratio	2.42	3.67	3	1.49
Head/neck ratio	4.49	5.5	5.15	5.3
Neck/trochanter ratio	0.54	0.67	0.58	0.28

stumbling resulted in densification of the whole femur including the femoral neck area, where the femur is prone to fracture.

In this study, constant peak loads during selected activities were used for the purpose of bone remodeling stimulus. However in the daily life, loads are time dependent and are applied on a cyclic basis on the bone and it would be more realistic to use time-dependent loads [6,22]. On the other hand, in the real life, a mixture of many different types of loadings is exerted on the bone. In other words, the internal structure of the bone is not governed by one or two type of loading patterns. The internal structure of the bone would be better predicted if the loading profiles have the potential to address as much routine activities as possible. Besides these limitations, the proposed model shows a promising means to understand the effects of different individual loading patterns on the bone density. Furthermore, the proposed model provides insight into selecting exercises which can be used to strengthen bone at different regions of the proximal femur.

Acknowledgment

The authors would like to acknowledge Dr. Miguel Perez for providing helpful feedback on the manuscript. This work has been supported by the Qatar National Research Foundation (QNRF) under Award No. NPRP 5-086-2-031.

References

[1] Parfitt, A., 1983, "The Physiologic and Clinical Significance of Bone Histomorphometric Data," *Bone Histomorphometry: Techniques and Interpretation*, CRC, Boca Raton, FL, p. 143.
[2] Wolff, J., Maquet, P., and Furlong, R., 1986, *The Law of Bone Remodelling*, Springer, Berlin, Germany.
[3] Brekelmans, W., Poort, H., and Slooff, T., 1972, "A New Method to Analyse the Mechanical Behaviour of Skeletal Parts," Acta Orthop., **43**(5), pp. 301–317.
[4] Hart, R., Davy, D., and Heiple, K., 1984, "Mathematical Modeling and Numerical Solutions for Functionally Dependent Bone Remodeling," Calcif. Tissue Int., **36**(1), pp. S104–S109.
[5] Carter, D., Fyhrie, D., and Whalen, R., 1987, "Trabecular Bone Density and Loading History: Regulation of Connective Tissue Biology by Mechanical Energy," J. Biomech., **20**(8), pp. 785–794.
[6] Huiskes, R., Weinans, H., Grootenboer, H., Dalstra, M., Fudala, B., and Slooff, T., 1987, "Adaptive Bone-Remodeling Theory Applied to Prosthetic-Design Analysis," J. Biomech., **20**(11), pp. 1135–1150.
[7] Marzban, A., Canavan, P., Warner, G., Vaziri, A., and Nayeb-Hashemi, H., 2012, "Parametric Investigation of Load-Induced Structure Remodeling in the Proximal Femur," Proc. Inst. Mech. Eng., Part H, **226**(6), pp. 450–460.
[8] Bitsakos, C., Kerner, J., Fisher, I., and Amis, A. A., 2005, "The Effect of Muscle Loading on the Simulation of Bone Remodelling in the Proximal Femur," J. Biomech., **38**(1), pp. 133–139.
[9] Turner, A., Gillies, R., Sekel, R., Morris, P., Bruce, W., and Walsh, W., 2005, "Computational Bone Remodelling Simulations and Comparisons With DEXA Results," J. Orthop. Res., **23**(4), pp. 705–712.
[10] Boyle, C., and Kim, I. Y., 2011, "Three-Dimensional Micro-Level Computational Study of Wolff's Law via Trabecular Bone Remodeling in the Human Proximal Femur Using Design Space Topology Optimization," J. Biomech., **44**(5), pp. 935–942.
[11] Hambli, R., Lespessailles, E., and Benhamou, C.-L., 2013, "Integrated Remodeling-to-Fracture Finite Element Model of Human Proximal Femur Behaviour," J. Mech. Behav. Biomed. Mater., **17**, pp. 89–106.
[12] Fyhrie, D., and Carter, D., 1986, "A Unifying Principle Relating Stress to Trabecular Bone Morphology," J. Orthop. Res., **4**(3), pp. 304–317.
[13] Carter, D., Orr, T., and Fyhrie, D., 1989, "Relationships Between Loading History and Femoral Cancellous Bone Architecture," J. Biomech., **22**(3), pp. 231–244.
[14] Adachi, T., Tomita, Y., Sakaue, H., and Tanaka, M., 1997, "Simulation of Trabecular Surface Remodeling Based on Local Stress Nonuniformity," JSME Int. J. Ser. C, **40**(4), pp. 782–792.
[15] Adachi, T., Tsubota, K.-I., Tomita, Y., and Hollister, S. J., 2001, "Trabecular Surface Remodeling Simulation for Cancellous Bone Using Microstructural Voxel Finite Element Models," ASME J. Biomech. Eng., **123**(5), pp. 403–409.
[16] Beaupré, G., Orr, T., and Carter, D., 1990, "An Approach for Time-Dependent Bone Modeling and Remodeling—Theoretical Development," J. Orthop. Res., **8**(5), pp. 651–661.
[17] Cowin, S. C., 2001, *Bone Mechanics Handbook*, CRC, Boca Raton, FL.
[18] Keaveny, T. M., Morgan, E. F., Niebur, G. L., and Yeh, O. C., 2001, "Biomechanics of Trabecular Bone," Annu. Rev. Biomed. Eng., **3**(1), pp. 307–333.
[19] Sarikanat, M., and Yildiz, H., 2011, "Determination of Bone Density Distribution in Proximal Femur by Using the 3D Orthotropic Bone Adaptation Model," Proc. Inst. Mech. Eng., Part H, **225**(4), pp. 365–375.
[20] Miller, Z., Fuchs, M. B., and Arcan, M., 2002, "Trabecular Bone Adaptation With an Orthotropic Material Model," J. Biomech., **35**(2), pp. 247–256.
[21] Ashman, R., Rho, J., and Turner, C., 1989, "Anatomical Variation of Orthotropic Elastic Moduli of the Proximal Human Tibia," J. Biomech., **22**(8), pp. 895–900.
[22] Turner, C. H., Rho, J., Takano, Y., Tsui, T. Y., and Pharr, G. M., 1999, "The Elastic Properties of Trabecular and Cortical Bone Tissues are Similar: Results From Two Microscopic Measurement Techniques," J. Biomech., **32**(4), pp. 437–441.
[23] Marzban, A., Nayeb-Hashemi, H., and Vaziri, A., 2013, "Numerical Simulation of Load-Induced Bone Structural Remodelling Using Stress-Limit Criterion," Comput. Methods Biomech. Biomed. Eng., **18**(3), pp. 259–268.
[24] Keyak, J. H., Rossi, S. A., Jones, K. A., and Skinner, H. B., 1997, "Prediction of Femoral Fracture Load Using Automated Finite Element Modeling," J. Biomech., **31**(2), pp. 125–133.
[25] Ethier, C. R., and Simmons, C. A., 2007, *Introductory Biomechanics: From Cells to Organisms*, Cambridge University, Cambridge, UK.
[26] Couteau, B., Labey, L., Hobatho, M., Vander Sloten, J., Arlaud, J., and Brignola, J., 1999, "Validation of a Three Dimensional Finite Element Model of a Femur With a Customized Hip Implant," Comput. Methods Biomech. Biomed. Eng., **2**(2), pp. 147–154.
[27] Taylor, W., Roland, E., Ploeg, H., Hertig, D., Klabunde, R., Warner, M., Hobatho, M., Rakotomanana, L., and Clift, S., 2002, "Determination of Orthotropic Bone Elastic Constants Using FEA and Modal Analysis," J. Biomech., **35**(6), pp. 767–773.
[28] Heller, M., Bergmann, G., Kassi, J.-P., Claes, L., Haas, N., and Duda, G., 2005, "Determination of Muscle Loading at the Hip Joint for Use in Pre-Clinical Testing," J. Biomech., **38**(5), pp. 1155–1163.
[29] El'Sheikh, H., MacDonald, B., and Hashmi, M., 2003, "Finite Element Simulation of the Hip Joint During Stumbling: A Comparison Between Static and Dynamic Loading," J. Mater. Process. Technol., **143**, pp. 249–255.
[30] Bergmann, G., Graichen, F., and Rohlmann, A., 1993, "Hip Joint Loading During Walking and Running, Measured in Two Patients," J. Biomech., **26**(8), pp. 969–990.
[31] Lennon, A., McCormack, B., and Prendergast, P., 1998, "Development of a Physical Model of a Cemented Hip Replacement for Investigation of Cement Damage Accumulation," J. Biomech., **31**(Suppl. 1), p. 129.
[32] Homminga, J., McCreadie, B., Ciarelli, T., Weinans, H., Goldstein, S., and Huiskes, R., 2002, "Cancellous Bone Mechanical Properties From Normals and Patients With Hip Fractures Differ on the Structure Level, Not on the Bone Hard Tissue Level," Bone, **30**(5), pp. 759–764.
[33] Keyak, J. H., and Falkinstein, Y., 2003, "Comparison of In Situ and In Vitro CT Scan-Based Finite Element Model Predictions of Proximal Femoral Fracture Load," Med. Eng. Phys., **25**(9), pp. 781–787.
[34] Nazarian, A., von Stechow, D., Zurakowski, D., Müller, R., and Snyder, B. D., 2008, "Bone Volume Fraction Explains the Variation in Strength and Stiffness of Cancellous Bone Affected by Metastatic Cancer and Osteoporosis," Calcif. Tissue Int., **83**(6), pp. 368–379.
[35] Van Rietbergen, B., Kabel, J., Odgaard, A., and Huiskes, R., 1997, "Determination of Trabecular Bone Tissue Elastic Properties by Comparison of Experimental and Finite Element Results," *Material Identification Using Mixed Numerical Experimental Methods*, Springer, Netherlands, pp. 183–192.
[36] Ladd, A. J., Kinney, J. H., Haupt, D. L., and Goldstein, S. A., 1998, "Finite-Element Modeling of Trabecular Bone: Comparison With Mechanical Testing and Determination of Tissue Modulus," J. Orthop. Res., **16**(5), pp. 622–628.

[37] Hou, F. J., Lang, S. M., Hoshaw, S. J., Reimann, D. A., and Fyhrie, D. P., 1998, "Human Vertebral Body Apparent and Hard Tissue Stiffness," J. Biomech., **31**(11), pp. 1009–1015.
[38] Kabel, J., van Rietbergen, B., Dalstra, M., Odgaard, A., and Huiskes, R., 1999, "The Role of an Effective Isotropic Tissue Modulus in the Elastic Properties of Cancellous Bone," J. Biomech., **32**(7), pp. 673–680.
[39] Baum, T., Carballido-Gamio, J., Huber, M., Müller, D., Monetti, R., Räth, C., Eckstein, F., Lochmüller, E., Majumdar, S., and Rummeny, E., 2010, "Automated 3D Trabecular Bone Structure Analysis of the Proximal Femur—Prediction of Biomechanical Strength by CT and DXA," Osteoporosis Int., **21**(9), pp. 1553–1564.
[40] Huber, M. B., Carballido-Gamio, J., Bauer, J. S., Baum, T., Eckstein, F., Lochmuller, E. M., Majumdar, S., and Link, T. M., 2008, "Proximal Femur Specimens: Automated 3D Trabecular Bone Mineral Density Analysis at Multidetector CT—Correlation With Biomechanical Strength Measurement 1," Radiology, **247**(2), pp. 472–481.